Science Translational Medicine AAAS

# Close-Field Electroporation Gene Delivery Using the Cochlear Implant Electrode Array Enhances the Bionic Ear

Jeremy L. Pinyon *et al.*

*Sci Transl Med* **6**, 233ra54 (2014);
DOI: 10.1126/scitranslmed.3008177

Editor's Summary

## Can You Hear Me Now?

Hearing loss affects millions worldwide. Sensorineural hearing loss, in particular, typically follows the loss of cochlear hair cells—specialized cells in the inner ear that help convert acoustic vibrations into nerve impulses, a process that allows you to hear. Cochlear implants, or "bionic ears," have been incredibly useful for deaf individuals; however, improvements in sound quality and range of environments where the implant can be used are desired. In this issue, Pinyon and colleagues worked to improve upon existing implants by simultaneously delivering a neurotrophic factor that can regenerate auditory nerves and, in turn, restore hearing.

The authors coined their approach "close-field electroporation." An electrode array inserted into the cochlea of guinea pigs delivered brief, intense electrical pulses to surrounding tissue. This led to electroporation—basically, a temporary opening of the cell membrane—which allowed passage of genetic material into the mesenchymal cells lining the scala tympani. Once inside the cells' nuclei, the gene construct produced brain-derived neurotrophic factor (BDNF), a protein in humans that is considered to be a nerve growth factor. Electroporation-mediated *BDNF* gene delivery drove regeneration of neurites in the cochlea, leading to restoration of hearing in a deafened guinea pig model (animals with hair cells destroyed). Because cochlear implants are already routinely used in patients, with further optimization of electroporation, it is possible that including gene therapy could restore hearing loss and improve the quality of hearing in deaf individuals.



*Science Translational Medicine* (print ISSN 1946-6234; online ISSN 1946-6242) is published weekly, except the last week in December, by the American Association for the Advancement of Science, 1200 New York Avenue NW, Washington, DC 20005. 

GENE THERAPY

# Close-Field Electroporation Gene Delivery Using the Cochlear Implant Electrode Array Enhances the Bionic Ear

**Jeremy L. Pinyon, Sherif F. Tadros, Kristina E. Froud, Ann C. Y. Wong, Isabella T. Tompson, Edward N. Crawford, Myungseo Ko, Renée Morris, Matthias Klugmann, Gary D. Housley***

**The cochlear implant is the most successful bionic prosthesis and has transformed the lives of people with profound hearing loss. However, the performance of the "bionic ear" is still largely constrained by the neural interface itself. Current spread inherent to broad monopolar stimulation of the spiral ganglion neuron somata obviates the intrinsic tonotopic mapping of the cochlear nerve. We show in the guinea pig that neurotrophin gene therapy integrated into the cochlear implant improves its performance by stimulating spiral ganglion neurite regeneration. We used the cochlear implant electrode array for novel "close-field" electroporation to transduce mesenchymal cells lining the cochlear perilymphatic canals with a naked complementary DNA gene construct driving expression of brain-derived neurotrophic factor (*BDNF*) and a green fluorescent protein (*GFP*) reporter. The focusing of electric fields by particular cochlear implant electrode configurations led to surprisingly efficient gene delivery to adjacent mesenchymal cells. The resulting *BDNF* expression stimulated regeneration of spiral ganglion neurites, which had atrophied 2 weeks after ototoxic treatment, in a bilateral sensorineural deafness model. In this model, delivery of a control *GFP*-only vector failed to restore neuron structure, with atrophied neurons indistinguishable from unimplanted cochleae. With BDNF therapy, the regenerated spiral ganglion neurites extended close to the cochlear implant electrodes, with localized ectopic branching. This neural remodeling enabled bipolar stimulation via the cochlear implant array, with low stimulus thresholds and expanded dynamic range of the cochlear nerve, determined via electrically evoked auditory brainstem responses. This development may broadly improve neural interfaces and extend molecular medicine applications.**

## INTRODUCTION

Hearing loss is the most prevalent sensory disability, stemming from genetics, environmental factors, particularly noise, ototoxicity, and aging (*1*–*3*). The cochlear implant bionic prosthesis has helped people suffering profound hearing loss and, more broadly, has fostered development of the field of implantable bionic interfaces. Cochlear implants use real-time processing of sound into frequency components, which are mapped to particular electrodes along the cochlear implant array as brief current pulses that recruit subpopulations of spiral ganglion neurons (SGNs) that form the auditory nerve. Advances in cochlear implant performance have benefitted from innovative engineering and computational capabilities of the peripheral components (*4*). However, the neural interface itself, typically consisting of an array of small platinum electrodes (each ~500 μm in diameter), has remained largely unchanged (*5*).

In normal-hearing subjects, the cochlea is tonotopically mapped so that the sensory hair cells at the base of the cochlea encode the highest-frequency sounds and progressively lower frequencies are detected toward the apex. With sensorineural hearing loss, the sensory hair cells and their supporting cells in the organ of Corti are lost, and the SGNs atrophy. The dieback of the auditory nerve is attributed to the loss of neurotrophin support, principally brain-derived neurotrophic factor (BDNF) and neurotrophin 3 (NT3), from the organ of Corti, signaled via tyrosine kinase receptors (Trks) expressed by the SGNs (*6*–*8*). The placement of a line of electrodes within scala tympani, a fluid chamber in the cochlea, enables the cochlear implant to electrically stimulate the SGNs and restore a facsimile of hearing. The number of electrodes is constrained by current spread associated with stimulation of the atrophied SGN somata localized behind the boney modiolar wall of the cochlea (*5*). Thus, a neural gap exists between the cochlear implant and the SGN somata, which necessitates the use of monopolar stimulation with current return via an electrode external to the cochlea. This subverts the tonotopic mapping of cochlear sound coding. Thus, cochlear implant recipients rely on the plasticity of the central auditory processing in the brain to translate the broad neuronal recruitment into speech perception, with concomitantly poor pitch perception (*4*). Closing the neural gap between the cochlear implant and the target sensory neurons offers the opportunity to surmount current biophysical limitations of SGN recruitment (*5*).

Proof-of-principle studies using viral vector–based gene therapy to treat deafness have revealed considerable potential for restoring hearing function in animal models. Hearing loss of genetic origin has been reversed in the vesicular glutamate transporter-3–null mouse model, with adeno-associated virus *VGlut3* gene therapy targeting the neonatal inner hair cell synapses (*9*). Cochlear expression of the transcriptional regulator *Atoh1* (also known as *Math1*) has driven transfection of supporting cells in the organ of Corti into new hair cells (*10*), which are innervated de novo by spiral ganglion neurites, to recover hearing function (*11*). Restoration of hair cells via transdifferentiation is not possible with profound hearing loss owing to degeneration of supporting cells. However, neuronal atrophy has been reversed and peripheral spiral ganglion neurites have been restored, resulting in better cochlear implant performance in guinea pigs using BDNF and NT3 therapy

Translational Neuroscience Facility and Department of Physiology, School of Medical Sciences, University of New South Wales, UNSW Australia, Sydney, New South Wales 2052, Australia.
*Corresponding author: E-mail: g.housley@unsw.edu.au

(*12*–*14*). Although viral vector gene therapy approaches show promise, clinical translation will need to address delivery, targeting, and safety constraints (*2*).

Electroporation offers an alternative pathway for cochlear gene delivery, but in the conventional "open-field" configuration, the need to place separate electrodes across the boney cochlear compartments precludes effective cell transfection. Such open-field electroporation has previously been directed to studying cell signaling in cochlear neurodevelopment. For example, transfection of murine cochlear cells has been achieved using paddle-style electrodes and injection of an *Atoh1* gene construct into the mouse embryo otic placode in utero (*15*). Open-field electroporation has also been used for in vitro transfection of rodent embryonic and neonatal cochlear sensory epithelium explant tissue (*16*–*18*).

Here, we investigated whether the cochlear implant electrode array could be used to generate localized high electric fields for electroporation-mediated gene delivery in a deafened adult guinea pig cochlea. This "close-field" electroporation (CFE), using local current paths between adjacent nodes of an array of electrodes, achieved high-efficiency *BDNF* gene delivery in a spatially prescribed zone. The resultant *BDNF* expression drove regeneration of the SGN neurites to close apposition with the cochlear implant electrodes. The nerve fibers were then able to be recruited by local bipolar stimulation, with minimal current spread. The findings therefore pave the way for integration of gene therapy into the cochlear implantation surgery, where a neurotrophin-encoding plasmid DNA can be introduced via a few brief electrical pulses, to produce directed regeneration of the auditory nerve that improves the functionality of the bionic interface.

## RESULTS

### Ex vivo cochlear gene delivery

An ex vivo model was developed to establish the potential of cochlear implant–mediated CFE gene delivery. We developed a bicistronic gene cassette (CMVp-*BDNF*-IRES-*GFP*nls) using the cytomegalovirus (CMV) promoter to drive expression of FLAG-tagged *BDNF* and, via an internal ribosome entry site (IRES) element, a green fluorescent protein (*GFP*) reporter with a nuclear localization site sequence (Fig. 1A). This circular complementary DNA (cDNA) plasmid was microinjected into the perilymphatic fluid spaces (scala tympani and scala vestibuli) of normal intact guinea pig cochleae. An eight-node cochlear implant electrode array was then inserted into the basal turn of the cochlea via the round window (Fig. 1, B and C). The array was configured as either an "alternating" configuration of anodes (+) and cathodes (−) or a "tandem" array where four adjacent nodes were wired in parallel as the anode (distal end of the array), and the other nodes provided a common cathode (Fig. 1D).

Cells were transfected with the gene cassette across a voltage range (4 V, up to 100 V; 5 to 50 pulses, 50-ms duration) in 85 experiments (table S1). GFP reporter fluorescence was prominent in mesenchymal cells lining the scala tympani and scala vestibuli, including the perilymphatic surface of Reissner's membrane (Fig. 2, A and B), and

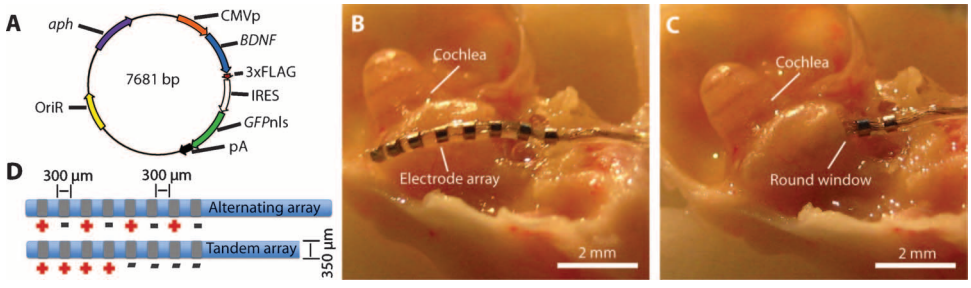


**Fig. 1. Gene therapy construct and CFE configuration.** (**A**) CMVp-*BDNF*-IRES-*GFP*nls plasmid [7681 base pairs (bp)]. The *BDNF* and *GFP*nls coding regions are transcribed simultaneously but translated as separate proteins via an IRES. pA, SV40n polyadenylation site; OriR, origin of replication; *aph*, kanamycin selection. (**B** and **C**) In ex vivo experiments, the guinea pig cochlea was exposed (B) and the eight-node cochlear implant was inserted into scala tympani via the round window (C). (**D**) CFE cochlear implant electrode array configurations.

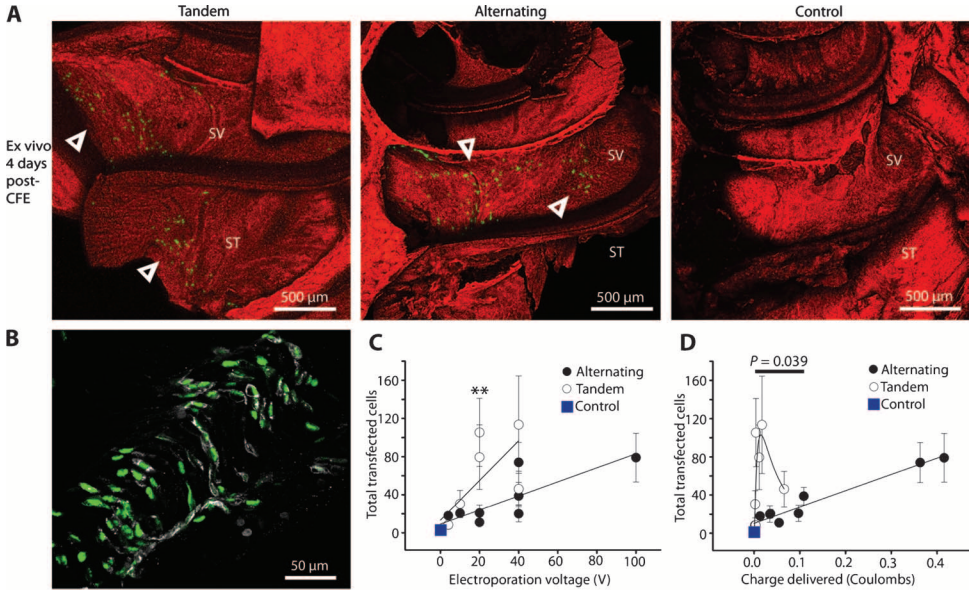


**Fig. 2. Ex vivo CFE.** (**A**) Confocal projected images of the distribution of transfected mesenchymal cells (nuclear-localized GFP) lining the perilymphatic compartments [scala tympani (ST) and scala vestibuli (SV)] of the cochlea (white arrowheads). Red is autofluorescence to resolve structure. Tandem configuration example: 5 × 20-V pulses. Alternating configuration: 20 × 40-V pulses. Control: *BDNF-GFP* plasmid loading with cochlear implant, but without CFE. (**B**) BDNF production in mesenchymal cells confirmed by anti-FLAG immunofluorescence (white) coincident with the GFP nuclear labeling (green). (**C** and **D**) Effect of voltage (C) and charge (D) on electroporation efficiency ($GFP^+$ cells) for the two different CFE modalities. Data are means ± SEM with best-fit linear trend lines shown. Multiple data points at each voltage level reflect variation in number of pulses (see table S1 for experimental numbers). For (C), $^{**}P = 0.005$, ANOVA, Holm-Sidak all-pairwise comparison. For (D), $^{*}P = 0.039$, Mann-Whitney rank sum test.

was maintained for the duration of organotypic cultures (3 to 4 days). The GFP-positive cells were confined to the basal turn region, within ~1 mm of the array, consistent with spatially constrained electroporation of the cells. CFE was effective from as low as 4 V (combined mean ± SEM = 9.5 ± 1.8 cells per cochlea, $n = 8$; $P = 0.017$, unpaired $t$ test) (table S1). In comparison, control experiments where free DNA was introduced into the cochlea without electroporation yielded minimal GFP-positive cell counts (mean ± SEM = 2.8 ± 0.5 cells per cochlea; $n = 5$ cochleae) (Fig. 2C). Expression of *BDNF* by transfected cells was confirmed by anti-FLAG immunolabeling (Fig. 2B).

The tandem electrode array configuration demonstrated greater gene delivery efficiency than the alternating array configuration, with an asymmetric optimum in the lower range of applied voltages (~20 V) (Fig. 2C) and, from resistance measurements during the voltage steps, a minimum effective charge delivery of ~0.04 C (Fig. 2D). Up to 310 $GFP^+$ cells were achieved (mean = 105.4 ± 35.7 cells per cochlea; $n = 8$), with five 20 V pulses lasting 50 ms each, with no increase with additional pulses. This equated to a charge density per pulse of ~60 $mC/cm^2$ on the four platinum ring anodes (table S1). In contrast, the alternating configuration provided a linear increase in transfection efficiency with increasing voltage to the highest test level and charge delivery, for example, 20.8 ± 8.4 cells at 20 V, 20 pulses ($n = 6$) to 79.0 ± 25.5 cells ($n = 3$) at 100 V, 5 pulses (0.42 C total charge). Overall, there was a significantly greater transfection efficiency with the tandem versus alternating array configurations between 0.002 and 0.109 C [$P = 0.017$, ranked one-way analysis of variance (ANOVA)] (Fig. 2D).

### In vivo cochlear gene delivery transfection efficiency and expression longevity

The cochlear implant was surgically inserted into anesthetized, normal-hearing guinea pigs for CFE gene delivery (fig. S1 and table S2). All cochleae in this initial in vivo study were fixed 3 to 4 days after electroporation. In vivo CFE using the optimum 20- to 40-V range (Fig. 3 and table S2) yielded comparable GFP-expressing cells to the corresponding ex vivo experiments (Fig. 2 and table S1). Middle and apical regions of the cochlea were devoid of $GFP^+$ cells in these in vivo experiments (Fig. 3, A and B). Tandem CFE produced greater numbers of transfected mesenchymal cells in vivo than did alternating CFE (Fig. 3C). There was no significant difference between the numbers of transfected cells ex vivo and in vivo using the tandem 20-V, 5-pulse protocol ($P = 0.232$, Mann-Whitney rank sum test). Cryosectioning of electroporated cochleae revealed that the transfection was effectively constrained to mesenchymal cells lining scala tympani and scala vestibuli (Fig. 3D). Hair cells and supporting cells of the organ of Corti, or other cell types facing scala media, were not transfected.

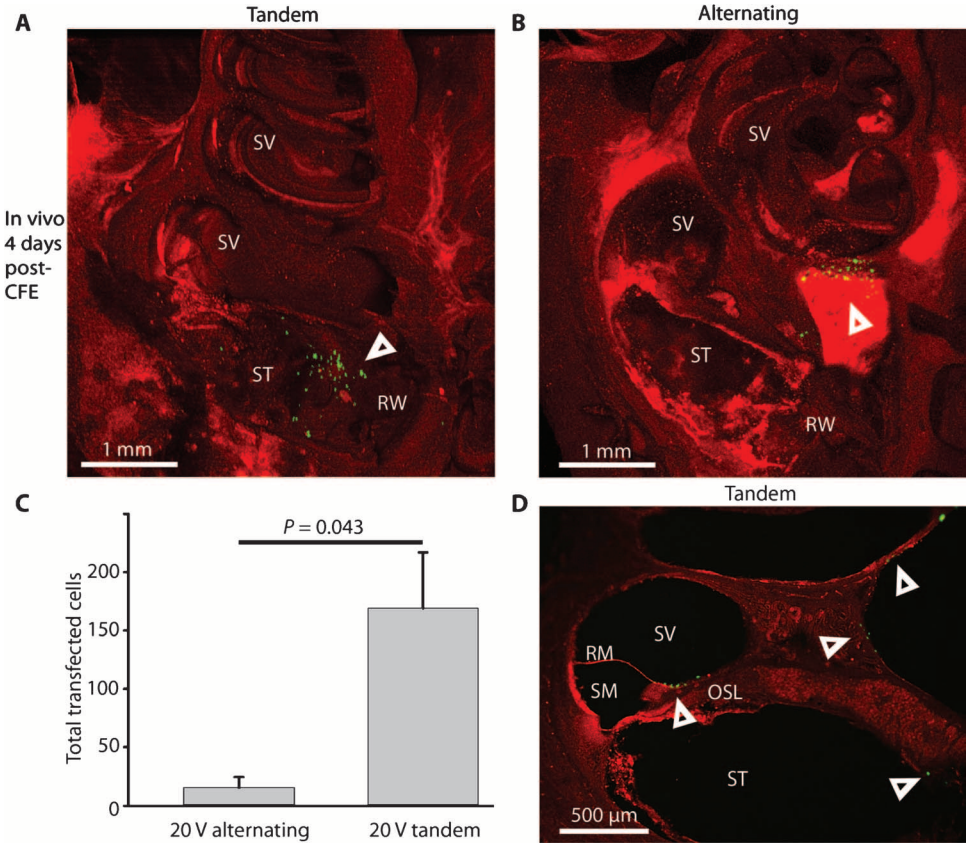


**Fig. 3. In vivo CFE in guinea pigs.** (**A** and **B**) Five pulses of 20 V each were delivered by CFE to the basal turn region of cochleae in either tandem (A) or alternating (B) electrode configuration. Transduced mesenchymal cells are green ($GFP^+$) in the perilymphatic compartments [scala tympani (ST) and scala vestibuli (SV)], indicated by white arrowhead. RW, round window. Autofluorescence (red) provides structural detail. (**C**) Transfection efficiency in the two different configurations. Data are means ± SEM ($n = 7$ tandem, 4 alternating). $P$ values were determined by $t$ test. (**D**) Cryosection (50 µm) identifying the transfected mesenchymal cells ($GFP^+$) lining the perilymphatic compartments, particularly the modiolar wall (arrowheads). OSL, osseous spiral lamina. Images in (A), (B), and (D) are representative of the 11 animals used for 20-V pulses [data shown in (C)] and for an additional 5 animals used in the alternating configuration with 40-V pulses (table S2).

Maximum transfection efficiency in vivo using the tandem array configuration was determined in three experiments (20 V, 5 pulses) 4 days after CFE. These experiments yielded 179 to 373 $GFP^+$ cells. Regions of interest that included at least 100 cells within the imaging field were analyzed for GFP and 4′,6-diamidino-2-phenylindole (DAPI) fluorescence. The average proportion of double-labeled nuclei in mesenchymal cells was 42.5 ± 3.3% (maximum transfection efficiency). No $GFP^+$ cells were detected in two control experiments of electroporation with a *GFP*-null vector. Two controls, where the left cochlea was perfused with the *GFP*-expressing *BDNF* plasmid followed by insertion of the electrode array, without electroporation, resulted in six and seven $GFP^+$ cells, respectively, 4 days after surgery (table S2).

Longevity of expression of the gene construct was observed for several weeks after CFE. In one guinea pig, where the cochlea

was analyzed 3 weeks after gene delivery, a total of 11 $GFP^+$ mesenchymal cells in seven 50-μm sections were localized to the basal turn region within scala tympani. No quantitative analysis was undertaken with additional animals at this time point, but the drop-off in expression around this time was confirmed in two cochleae examined 6 weeks after gene delivery (eight $GFP^+$ cells evident in only one hemisectioned cochlea), and no GFP expression was detected in cochleae from four animals at 10 weeks after gene delivery. GFP signal extending for up to 6 weeks suggests mRNA translation beyond the immediate gene delivery period.

### *BDNF* gene therapy in a deafened guinea pig model

Further in vivo experiments were carried out in a deafened guinea pig model. Animals were deafened using a kanamycin-furosemide ototoxic treatment to selectively remove the sensory hair cells, where the peripheral neurites of the SGN showed substantial degeneration within the osseous spiral lamina, and the SGN somata undergo atrophy (figs. S2 and S3). The deafened guinea pig organ of Corti typically exhibited progressive flattening of the sensory epithelium due to the loss of hair cells and supporting cells (fig. S2). Although interanimal variability in progression of SGN atrophy and loss has been reported with this ototoxic deafening procedure (*19*), our data were consistent with regard to substantial loss of neurites in the osseous spiral lamina at the 2-week post-deafening time point. At this time point, therapeutic *BDNF* cDNA was delivered via the cochlear implant array.

*BDNF* gene therapy led to regeneration of neurite processes that extended out through the osseous spiral lamina, with side branching

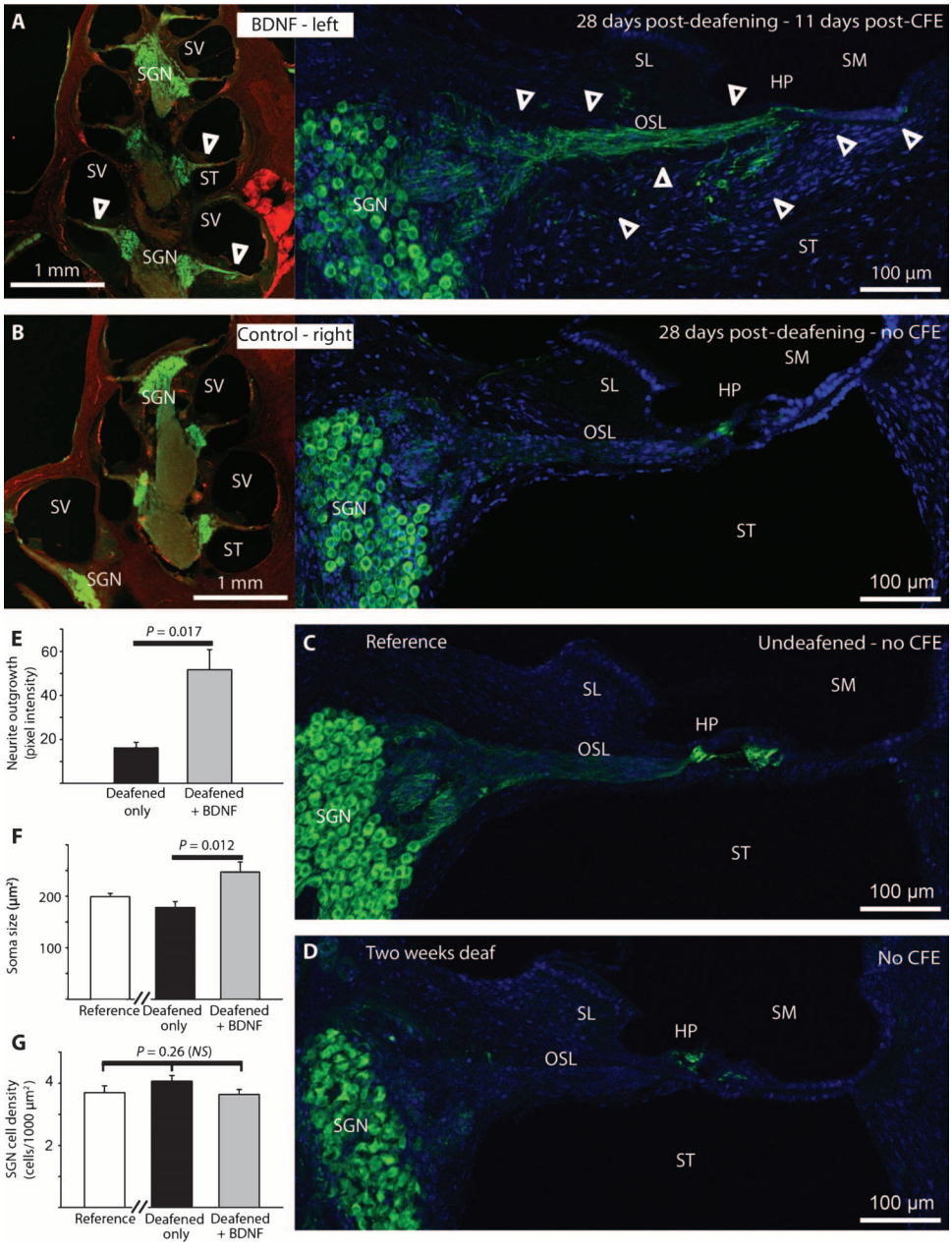


**Fig. 4. CFE mediates *BDNF* gene therapy in deafened guinea pig cochleae.** (**A** and **B**) *BDNF* gene therapy (A) and control cochleae (B) from a guinea pig deafened by ototoxicity, then 2 weeks later provided with CFE gene delivery to the left cochlea. Regeneration of SGNs (type III β-tubulin in green) is evident in the left cochlea (alternating array configuration; 40 V, 20 pulses) at 11 days after CFE. Restored neurites in the osseous spiral lamina (OSL) extended beyond the habenula perforata (HP) and branched into scala tympani (ST), as indicated by arrowheads. SL, spiral limbus; SM, scala media (endolymph); SV, scala vestibuli. (B) Control (right) cochlea from the same guinea pig in (A) showing the absence of peripheral neurites in the osseous spiral lamina and atrophy of the SGN somata. Right-side images in (A) and (B) provide detail of the basal turn region. Red is autofluorescence to show cochlear structure. Blue is DAPI nuclear staining. Images are representative of four animals (see also fig. S4). (**C** and **D**) SGN (β-tubulin immunofluorescence) in a cryosection from a reference (nondeafened) guinea pig cochlea (C) and from a cochlear cryosection 2 weeks after ototoxic deafening (D). (**E**) Neurite regeneration with gene therapy measured as β-tubulin immunofluorescence (pixel intensity per square micrometer) within the osseous spiral lamina 1 to 3 weeks after gene therapy (see also fig. S4). (**F** and **G**) Cross-sectional somata size (F) and packing densities of the SGN cell soma within Rosenthal's canal (G) of *BDNF*-treated cochleae compared with untreated cochleae of deafened guinea pigs and untreated, undeafened cochleae. Data are means ± SEM ($n$ = 4 per group). $P$ values in (E) and (F) were determined by paired $t$ tests. $P$ value in (G) was determined by ANOVA. NS, not significant.

through the modiolar wall via micropores (canaliculi perforantes), with most fibers reaching the habenula perforata, before descending through the basilar membrane into the scala tympani region (Fig. 4A). Neurite regeneration occurred from the basal turn (the site of mesenchymal cell transfection) to the mid-turn region of the *BDNF*-treated cochleae (Fig. 4A). This likely reflects diffusion of the secreted recombinant BDNF within the perilymph. Both alternating (40 V, 20 × 50-ms pulses; $n$ = 3) and tandem configuration CFE (20 V, 5 × 50-ms pulses; $n$ = 1) *BDNF* gene delivery to the left cochlea led to regeneration of the peripheral spiral ganglion neurites and increased the size of SGN somata compared with the untreated (right) cochleae of deafened guinea pigs (Fig. 4, A and B, and fig. S4). This reversal of SGN atrophy by gene therapy was evident by comparison of the reference SGN state before the deafening procedure (Fig. 4C) with the atrophy evident 2 weeks after deafening (Fig. 4D), the point when gene delivery was undertaken. Images of immunolabeled cryosections were analyzed from 1 to 3 weeks after gene delivery, corresponding to 3 to 5 weeks after deafening.

Neuronal-specific type III β-tubulin immunofluorescence within the osseous spiral lamina region (basal turn) indicated significantly greater neurite outgrowth in the *BDNF*-treated animals (Fig. 4E and fig. S4). In addition, the average SGN soma size was about 40% larger in the *BDNF* gene therapy–treated versus untreated cochleae of the deafened animals (Fig. 4F). There was no difference in SGN density between either BDNF-treated and untreated cochleae in the deafened guinea pigs or the undeafened reference cochleae, suggesting that SGN survival was not significantly affected within the first 5 weeks after deafening ($P$ = 0.184, paired $t$ test, comparing SGN cell density between left and right cochleae; $P$ = 0.26, ANOVA across groups including the reference) (Fig. 4G).

Ectopic branching extended to the inner sulcus and outer sulcus–spiral ligament region, within scala media, with some variation in fiber extension into scala tympani (Fig. 5A) compared with extension along the basilar membrane to the spiral ligament (Fig. 5B). Extension of neurite outgrowth also occurred toward the spiral limbus, across the inner sulcus (Fig. 6, A and B). The control (right cochleae) showed no remnant fibers beyond the habenula perforata (Fig. 6C).

The presence of the Schwann cell marker aspartoacylase (ASPA) (*20*) indicated remyelination of regenerated neurites up to 12 weeks after deafening (10 weeks after *BDNF* delivery), including the ectopic processes within scala tympani and scala media (Fig. 6D). Anti-ASPA immunofluorescence was also evident in the osseous spiral lamina of the untreated cochleae, consistent with preservation of the glial satellite cells and retention of residual SGN fibers (Fig. 6D). These glial cells are responsible for the remyelination of the SGN fibers and demonstrate myelination to the tips of the ectopic neurite branches.

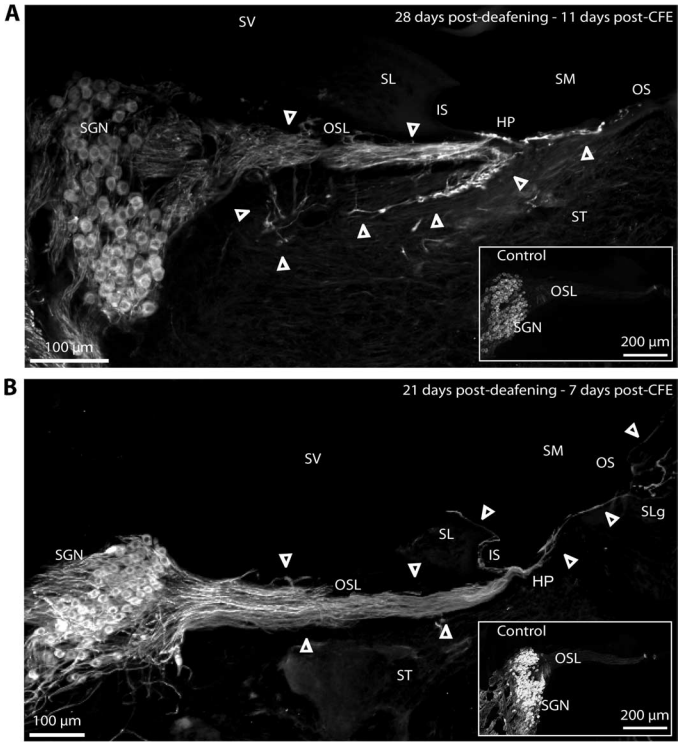


**Fig. 5. Regeneration of the SGN peripheral neurites in vivo after alternating configuration CFE *BDNF* gene therapy in deafened guinea pigs.** Animals were subjected to 20 pulses at 40 V. Confocal projected image reconstructions are of type III β-tubulin immunofluorescence in cochlear cryosections. (**A** and **B**) Detail variations in outgrowth of fibers (arrowheads) in the osseous spiral lamina (OSL), with ectopic branching of fibers into scala tympani (ST), both at the habenula perforata (HP) and through the modiolar wall via micropores called the canaliculi perforantes (A). Regenerated spiral ganglion neurites also projected past the remnant organ of Corti to the outer sulcus (OS) region and, in the example shown in (B), medially to the inner sulcus (IS). Insets in the bottom right corners show control (no CFE) cochleae from the same animals. SL, spiral limbus; SLg, spiral ligament; SM, scala media; SV, scala vestibuli.

## Enhanced cochlear implant performance

The functional effect of regeneration of the SGN neurites from CFE-mediated *BDNF* gene therapy was assessed in separate in vivo studies with the deafened guinea pig model. Electrically evoked auditory brainstem responses (eABRs) were measured 2 weeks after *BDNF-GFP* or *GFP*-only (control) gene delivery via CFE using the tandem array configuration (20 V, 5 × 50-ms pulses; $n$ = 5 for each), which was 4 weeks after the ototoxic treatment. With bipolar stimulation of the SGN via the tandem array configuration, the improvement in auditory brainstem pathway neural recruitment due to the *BDNF* gene therapy was evident from the lower current amplitudes needed to elicit threshold eABRs (Fig. 7A). The mean eABR stimulus threshold for the *BDNF* gene therapy group was <50% of the control group, with no overlap in threshold data (Fig. 7B). This improvement in cochlear implant performance can be assessed against the reference group, where cochlear implant stimulation was applied to normal-hearing guinea pigs (with auditory nerve and the sensory hair cells intact). This produced a mean eABR stimulus threshold (Fig. 7B) that was not significantly different from the deafened *BDNF* gene therapy group. The result suggests nominally optimum recovery of threshold, yet discounting possible augmentation of the response in this reference group due to electrophonic inner hair cell stimulation.

Baseline eABR thresholds were also determined 2 weeks after deafening, just before gene therapy (Fig. 7B). This was significantly higher than the *BDNF* gene therapy group 2 weeks later, after *BDNF* gene therapy, but significantly less than the *GFP*-only vector control group after 2-week expression of the *GFP*-only gene construct. These data indicate progressive deterioration in SGN function over time in the absence of *BDNF* gene therapy, consistent with the exacerbation of sensorineural hearing loss in this deafness model in the absence of neurotrophin treatment.

Complementing this, the dynamic range (growth function) of the eABR was significantly increased in the *BDNF* gene therapy treatment group (Fig. 7, C and D), with a considerable extension of the range of stimulus eliciting growth of the eABR compared with the *GFP* vector control group. Thus, *BDNF* gene therapy restored the cochlear nerve recruitment toward pretreatment levels. Overall, these results demonstrate a functional enhancement of the cochlear implant–neural interface arising from restoration of the peripheral SGN neurites after 2 weeks of CFE-mediated *BDNF* gene therapy.

## DISCUSSION

The development of the cochlear implant is currently limited by the neural gap between the atrophied SGNs and the electrode array. Delivery of therapeutics that may confer protection to the auditory nerve fibers during the implantation procedure, or indeed drive regeneration of the nerve fibers toward the electrodes, is necessary to improve the bionic ear. This study describes the development of CFE that uses multipolar configurations of the cochlear implant electrode array to generate focused electric fields for localized neurotrophin gene delivery in a guinea pig model. This integration of gene therapy into the cochlear implant procedure achieved focused expression of plasmid DNA encoding the neurotrophin BDNF. Production of BDNF promoted rapid directed regeneration of the auditory nerve fibers into close proximity with the cochlear implant electrodes, thereby closing the neural gap in the bionic interface and eliciting improved hearing sensitivity and dynamic range.

We used an ex vivo, organotypic culture model to establish the optimum conditions for CFE gene delivery before proceeding to the in vivo proof-of-principle studies. Electroporation is a well-established method for delivering drugs, proteins, and nucleic acids into cells (*21*, *22*). DNA migration across a cell membrane involves the electroporation of the plasma membrane by high electric fields, with an electrophoretic action for driving the negatively charged molecules across (*23*–*25*). Once inside the cell, DNA can migrate to the nucleus, where, in the case of circularized plasmid DNA, it remains extrachromosomal (episomal) and supports gene expression without the risk of mutagenesis that arises with integration. Here, we show that with electrode arrays, fields of sufficient intensity to transduce cells can be generated if current is passed between electrodes that are contiguous within an array. This provides highly localized transduction of the cells in the immediate vicinity of the array, as evidenced by GFP fluorescence within 24 hours. The ex vivo experiments demonstrated that the configuration of the electrodes within the array affected cell transfection, with the tandem configuration being most efficient. Amplitudes as low as 4 V yielded significant numbers of transfected cells. These studies also validated the production of the recombinant BDNF by the target mesenchymal cells. The selective transduction of mesenchymal cells is likely due to the limited diffusion of DNA from the perilymphatic compartment in the few minutes required for DNA loading and CFE.

The in vivo CFE experiments migrated the study from demonstration of targeted gene delivery and *BDNF* expression (by the mesenchymal cells adjacent to the electrodes) to confirmation of peripheral auditory nerve fiber regeneration, reversal of SGN somata atrophy, and remyelination

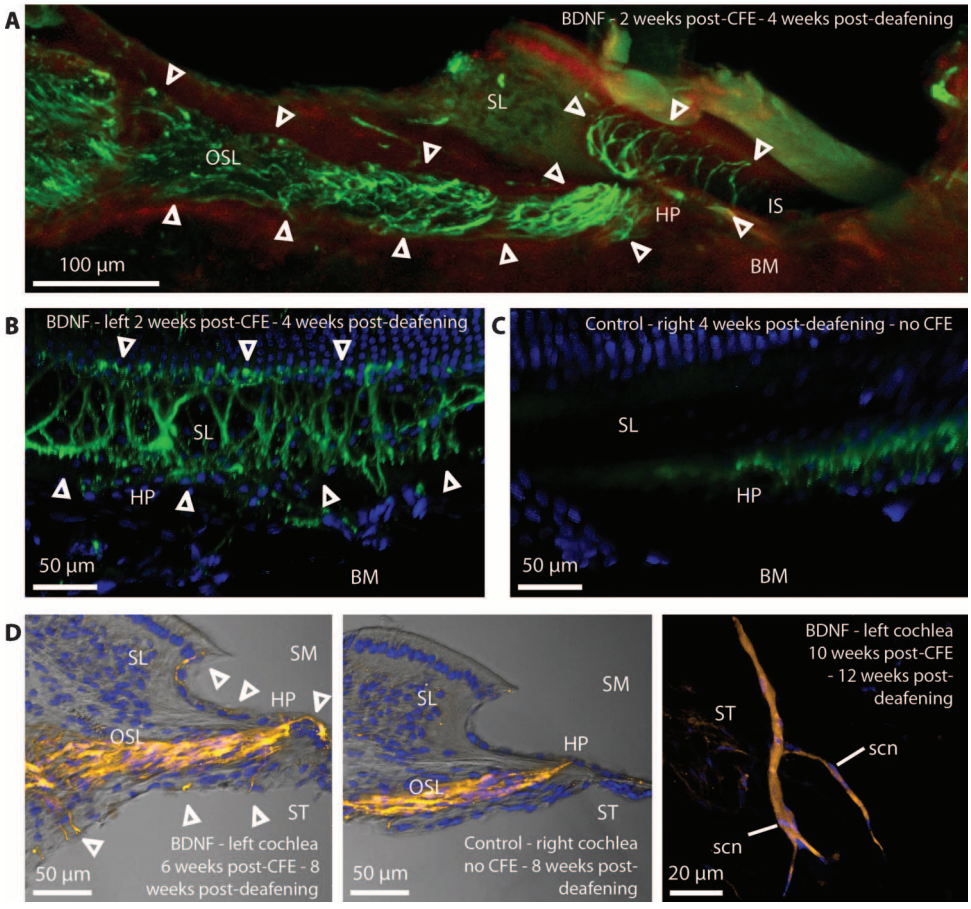


**Fig. 6. Neurite regeneration and remyelination after tandem configuration CFE *BDNF* gene therapy in deafened guinea pigs.** Animals were administered 5 pulses at 20 V each to deliver *BDNF*. (**A**) Type III β-tubulin immunofluorescence (green) of a hemisectioned cochlea 2 weeks after CFE ($n = 3$). Confocal three-dimensional reconstruction shows the SGN regeneration within the osseous spiral lamina (OSL), through the habenula perforata (HP) and extending to the inner sulcus (IS) region, under the lateral prominence of the spiral limbus (SL). Cochlear structure shown by autofluorescence (red). (**B**) Ectopic branching of the regenerated neurites bordering the spiral limbus within scala media from tissue shown in (A). Nuclear labeling (DAPI) is in blue. (**C**) Control (deafened, no gene therapy) cochlea from the same guinea pig. (**D**) Aspartoacylase immunofluorescence (orange) showing myelination of the regenerated neurites and ectopic branching 6 ($n = 2$) to 10 weeks ($n = 4$) after CFE. Images have transmitted light overlays for structural detail. DAPI-labeled nuclei show location of the satellite cells (scn) in the 10-week post-CFE image.

of the distal neurite processes. The extensive ectopic branching of the SGN neurites after BDNF therapy was reminiscent of the initial neurite extension that occurs when the SGN afferent fibers first innervate the cochlea searching for target hair cell synapses during development (*26*). The eABR assessment demonstrated that this auditory nerve regeneration lends restoration of nerve fiber recruitment thresholds to pre-deafness levels. The halving in eABR threshold achieved by *BDNF* gene therapy equates to the improved cochlear implant performance achieved in an earlier study in guinea pigs using direct BDNF drug delivery (*27*), whereas our absolute thresholds (hearing sensitivity) were about threefold less with bipolar stimulation.

Cochlear implants are typically enabled in monopolar stimulation mode to achieve the best auditory function, where individual electrodes within the implanted array are driven with current return via a common electrode located external to the cochlea (*5*). This provides the best recruitment of auditory neurons in the implant recipients because of the convoluted current path to the atrophied auditory neurons. In our studies, bipolar stimulation from adjacent nodes of the cochlear implant provided sensitive localized recruitment of the repaired auditory neurons. Translation of this outcome to a clinical setting would likely facilitate better sound perception in cochlear implant recipients via recruitment of smaller subpopulations of SGNs, as previously suggested (*5*). Currently, appreciation of tonal quality (for example, in music) is very limited, and the potential benefit that may accrue from more discrete recruitment of SGNs that we demonstrate here potentially makes tonal color and music appreciation a major potential gain (*28*).

The straightforward nature of the CFE gene delivery established here prompts consideration of whether neurotrophin gene therapy can be integrated into otological practice to enhance the performance of the "bionic ear." The eight-node array design used in the present study was developed for animal models. Given that the cochlear implant electrode arrays used clinically currently have up to 22 electrodes, the scalability of the electric field focusing will need to be pursued. Evaluation should also consider the current trend toward hybrid acoustic and electrode array implant devices, where residual low-frequency hearing is preserved and used (*29*). The incorporation of BDNF therapy into the cochlear implantation procedure via CFE may protect and preserve this residual sound transduction in the apical region of the cochlea. Alternative trophic factors may also prove useful in promoting directionality to neural outgrowth, which would maximize the sensitivity and selectivity of auditory neuron recruitment. For example, it has been shown that cochlear delivery of BDNF and NT3 proteins in combination is more effective in preserving SGN in sensorineural hearing loss models than either factor alone (*30*).

On the basis of the current studies, it is possible to envisage the ready integration of CFE-mediated *BDNF* therapy into cochlear implantation procedures, where an otologist could inject the naked cDNA gene construct into scala tympani just before insertion of the cochlear implant array, and then trigger a few brief electrical pulses via the array to transfect the mesenchymal cells close to the electrodes. Current cochlear implant devices have software-programmed current and pulse duration limitations as a safety constraint to prevent platinum electrode–based electrolysis with constant stimulation, typically <2-mA current and <1-ms stimulus duration. Nevertheless, the cochlear implant current supply and control circuitry are capable of levels and pulse durations approaching those used in the present study for effective directed gene delivery. For CFE, the minimum effective charge density on the platinum electrodes was ~25 mC/cm$^2$, with no roughness factor. Although this exceeds the safety limit of 210 μC/cm$^2$ nominally recommended for continuous stimulation, reflecting the pseudocapacity of the platinum

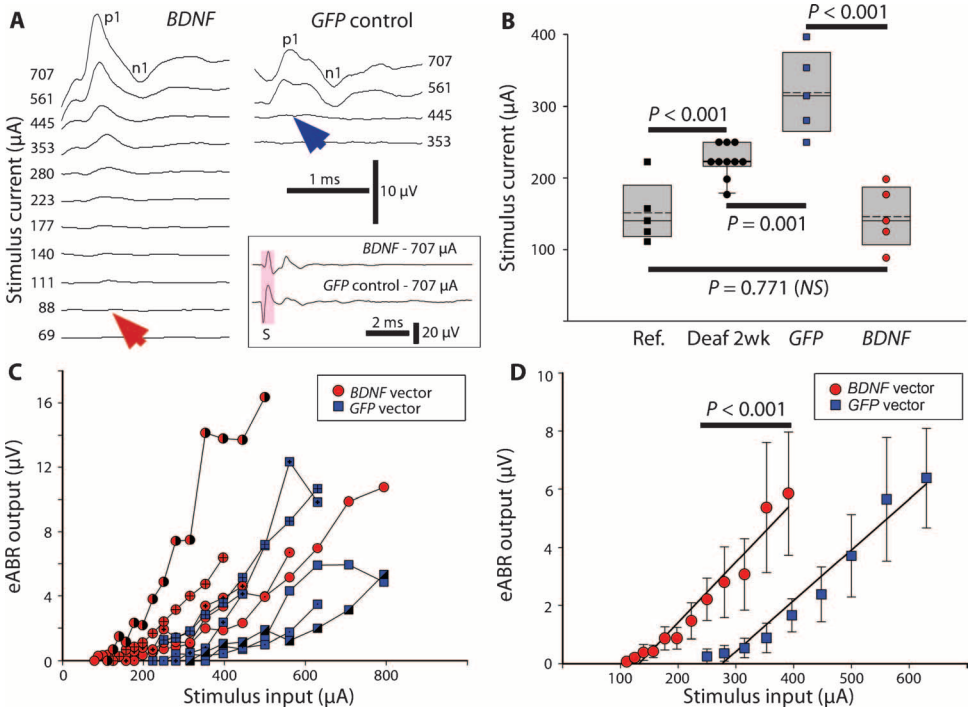


**Fig. 7. Enhanced cochlear implant performance 2 weeks after *BDNF* gene therapy in deafened guinea pigs.** Animals were deaf for 2 weeks before tandem configuration CFE, 5 pulses at 20 V. (**A**) eABR traces after *BDNF* gene therapy or CFE using a gutted plasmid (*GFP* control). Red and blue arrowheads show current stimulus needed to elicit a threshold response. Traces start after stimulus artifact. Representative full-length (10-ms) traces for the maximum stimulus levels are shown in the inset (S, stimulus artifact). (**B**) eABR thresholds of deafened guinea pigs compared with the *BDNF* treatment ($n = 5$) and control groups, including *GFP* control vector ($n = 5$). The reference group (Ref.) was implanted in normal-hearing guinea pigs ($n = 5$). The "Deaf 2wk" group was guinea pigs 2 weeks after chemical deafening ($n = 10$). Box plot solid lines show median, dashed lines show mean, and frame defines 25th and 75th percentiles. Data are individual animal hearing thresholds. *P* values were determined by ranked ANOVA with Holm-Sidak multiple pairwise comparisons. NS, not significant. (**C**) Individual eABR input-output functions for *BDNF*-treated deafened guinea pigs versus *GFP* vector–treated deafened controls. Data show the progressive growth in amplitude of the ABR p1-n1 wave as the stimulus current through the cochlear implant array is increased. Different symbols indicate different animals ($n = 5$ for each group). (**D**) Average eABR input-output growth functions from the data shown in (C) (means ± SEM). Linear best-fit trend lines are shown. *P* value was determined by repeated-measures two-way ANOVA for stimulus levels between 250 and 397 μA.

electrodes for reversible charge delivery (*31*), this upper limit for clinical use with continuous stimulation is not relevant to CFE, where only a few brief pulses over a period of seconds provides the gene delivery treatment. Hence, future technical development of the cochlear implant, or indeed other array-type interfaces, could certainly enable this gene delivery platform.

It was evident that *BDNF* expression in the cochlea waned 6 to 10 weeks after CFE. This may be due to the cDNA coding, including methylation of the CMV promoter, and future studies may consider the desirability of long-term episomal expression of plasmids that could be achieved using alternative hybrid promoters (*32*) and incorporation of viral coding elements, which have been shown to enable sustained expression of naked plasmid gene cassettes for many months (*33*). That said, the expression of the naked plasmid would still depend on the longevity of the mesenchymal cells, which is unknown. In this context, histological analysis showed no evidence of tissue damage associated with CFE, and fibrotic infiltration was evident without CFE. With CFE *BDNF* gene delivery, the fibrosis provided a scaffold that facilitated migration of the SGN neurites toward the electrodes, aiding in the reduction in the neural gap. This local gene therapy, if undertaken in conjunction with ongoing low-level electrical stimulation of the implant array, which is known to support SGNs (*34*), could ensure that the enhanced neural interface is sustained.

BDNF neurotrophin gene therapy has broad applicability to neural repair (*35*), but the electrode array–based CFE gene delivery developed here is not limited by particular gene constructs and overcomes constraints of other platforms. In this context, the charge delivery is considerably reduced over conventional open-field electroporation platforms, with the added benefit of minimal extraneous electrical stimulation of excitable tissues while achieving highly localized cell transfection. Safety concerns are considerably mitigated in comparison with viral vector–based gene therapy approaches, where uncontrolled spread of the virus can lead to undesirable off-target effects and immunological reactions may prove a barrier to implementation (*36*). CFE gene therapy also benefits from using naked DNA and lacks the packaging constraints associated with viral vectors so that plasmids well in excess of 7 kb can be used (our bicistronic *BDNF-GFP* gene cassette was 7.7 kb).

More broadly, the development of electrode array–based CFE gene delivery may not only improve the hearing of cochlear implant recipients but also find broader therapeutic applications, such as in conjunction with deep brain stimulation, which uses electrode arrays similar to the cochlear implant, to treat a range of neurological disorders, from Parkinson's disease to psychiatric disorders (*37*).

## MATERIALS AND METHODS

### Study design

The aim of the study was to determine how localized neurotrophin gene delivery could be achieved in the deafened guinea pig cochlea by generating focused electric fields using a cochlear implant electrode array of comparable design to the human clinical devices and to evaluate the functional impact of consequent sensory fiber regeneration. Three experimental series were performed: (i) ex vivo analysis of mesenchymal cell transfection where the cochlear tissue was placed into organotypic culture after in situ CFE in isolated cochleae, (ii) in vivo studies in normal-hearing guinea pigs to compare transfection efficiency with initial ex vivo data, and (iii) in vivo studies in deafened guinea pigs to determine efficacy of recombinant BDNF-mediated SGN regeneration and impact on cochlear implant performance. Animals were randomly assigned to treatment groups without blinding. Experimental numbers were based on power calculations from ANOVA with Holm-Sidak pairwise comparison that established differences between treatments, for example, electrode configurations in mid-range electrical pulse parameters for the ex vivo study. Procedures were approved by the University of New South Wales Animal Care and Ethics Committee and are described in the Supplementary Materials.

### Cochlear implant electrode array

This study used the cochlear implant electrode array to generate locally focused electric fields sufficient to electroporate cells adjacent to the array for DNA uptake. We define this variant of electroporation as CFE to differentiate this use of contiguous electrodes within an array from conventional open-field electroporation where the electrodes are separated by the target tissue or cell suspension. The electrode arrays were eight-node platinum ring arrays (part no. z60274, Cochlear Ltd.). The voltage pulses were generated with a commercial electroporator (CUY21, Nepa Gene). The eight nodes of the array were wired with alternative anodes (+) and cathodes (−) (alternating configuration) or with the distal four nodes as anodes and the proximal four nodes as cathodes (tandem configuration) (Fig. 1D).

### Vector preparation

The plasmid DNA was a bicistronic construct consisting of an expression cassette with a 3× FLAG-tagged *BDNF* element and a *GFP* reporter with a nuclear localization signal, driven by a CMV promoter (Fig. 1A). Details are given in the Supplementary Materials.

### Ex vivo and in vivo CFE

The plasmid DNA was pumped into the perilymphatic spaces (scala tympani and scala vestibuli) via the round window of the cochlea (20 μl at 2 μg/μl over ~40 s). The cochlear implant array was then inserted into scala tympani via the round window, and the electroporation proceeded with a limited number of 50-ms pulses (up to 50 at 1/s). Expression was analyzed by confocal laser scanning microscopy to detect GFP fluorescence from 16 hours onward. Immunofluorescence determined BDNF expression (anti-FLAG), neural regeneration (anti–β-tubulin), and remyelination (anti-aspartoacylase). Further details, including tissue processing, immunohistochemistry, and imaging, are described in the Supplementary Materials.

### Gene therapy in chronically implanted, deafened cochleae

Guinea pigs were deafened using a single combined ototoxic treatment of an intravenous infusion of a loop diuretic and subcutaneous administration of an aminoglycoside antibiotic [after (*38*, *39*)]. Under anesthesia as described above, furosemide (100 mg/kg, Frusemide, Troy Laboratories) was infused via the external jugular vein (in 3-ml normal saline over 6 min). This was followed by a subcutaneous injection of kanamycin sulfate (400 mg/kg, Sigma-Aldrich). After a 2-week recovery period, by which time there was substantial sensorineural hearing loss, the cochlear implant surgery was performed under isoflurane anesthesia, including CFE-mediated delivery of the *BDNF-GFP*, or control *GFP* plasmids as described. The connector for the cochlear implant was then sealed with paraffin film and sutured into a fistula located between the scapulae. Deafness was confirmed using acoustically driven ABR and distortion product otoacoustic emission (DPOAE) measurements via

a TDT systems III evoked potential workstation, including a Medusa optically coupled headstage (Tucker-Davis Technologies) within a sound-attenuating chamber (Sonora Technology) (*40*). Testing was performed before deafening and again 1 to 2 weeks after ototoxic treatment. ABR was determined at 2-, 4-, 8-, 16-, 24-, and 32-kHz tone pips (5 ms) and clicks (100 μs, alternating polarity), whereas DPOAE was tested at 6, 8, 16, 20, 24, and 28 kHz. ABR thresholds were tested to a maximum level of 90-dB sound pressure level (SPL), whereas DPOAE was evaluated to 70-dB SPL. Only animals lacking detectable ABR and DPOAE thresholds were used in the gene therapy experiments.

Functional evaluation of cochlear implant performance used electrically-evoked ABR under anesthesia, as described in the Supplementary Materials.

### Statistical analysis

Data in treatment groups were tested for normality (SigmaPlot 11, Systat Software Inc.). In cases where this test failed, the data were transformed by ranking which established normal distribution before analysis by ANOVA. Holm-Sidak post hoc multiple pairwise comparisons were performed, which included adjustment of the α value below 0.05 depending on the number of comparisons. For single comparisons between left (treated) and right (untreated) cochleae in the same animal, two-tailed paired *t* tests were undertaken. Where indicated, nonparametric analysis used the Mann-Whitney rank sum test. In graphs, error bars indicate ±SEM.

## SUPPLEMENTARY MATERIALS

www.sciencetranslationalmedicine.org/cgi/content/full/6/233/233ra54/DC1

Materials and Methods

Fig. S1. Micro–computed tomography of the guinea pig skull showing the cochlear implant array.

Fig. S2. Characterization of the guinea pig cochlear sensory epithelium degeneration after ototoxic treatment.

Fig. S3. Acoustically evoked ABRs to click stimuli in guinea pigs before and after ototoxic treatment.

Fig. S4. β-Tubulin immunofluorescence in cryosections demonstrating BDNF-mediated regeneration of spiral ganglion neurites in deafened guinea pig cochleae.

Table S1. Nuclear GFP-labeled mesenchymal cell counts arising from ex vivo cochlear CFE gene delivery.

Table S2. $GFP^+$ transfected mesenchymal cells after CFE in vivo.

Reference (*41*)

## REFERENCES AND NOTES


1. D. I. Nelson, R. Y. Nelson, M. Concha-Barrientos, M. Fingerhut, The global burden of occupational noise-induced hearing loss. *Am. J. Ind. Med.* **48**, 446–458 (2005).
2. J. R. Holt, L. H. Vandenberghe, Gene therapy for deaf mice goes viral. *Mol. Ther.* **20**, 1836–1837 (2012).
3. D. Yan, Y. Zhu, T. Walsh, D. Xie, H. Yuan, A. Sirmaci, T. Fujikawa, A. C. Wong, T. L. Loh, L. Du, M. Grati, S. M. Vlajkovic, S. Blanton, A. F. Ryan, Z. Y. Chen, P. R. Thorne, B. Kachar, M. Tekin, H. B. Zhao, G. D. Housley, M. C. King, X. Z. Liu, Mutation of the ATP-gated $P2X_2$ receptor leads to progressive hearing loss and increased susceptibility to noise. *Proc. Natl. Acad. Sci. U.S.A.* **110**, 2228–2233 (2013).
4. X. Li, K. Nie, N. S. Imennov, J. T. Rubinstein, L. E. Atlas, Improved perception of music with a harmonic based algorithm for cochlear implants. *IEEE Trans. Neural Syst. Rehabil. Eng.* **21**, 684–694 (2013).
5. S. J. O'Leary, R. R. Richardson, H. J. McDermott, Principles of design and biological approaches for improving the selectivity of cochlear implant electrodes. *J. Neural Eng.* **6**, 055002 (2009).
6. D. Ramekers, H. Versnel, W. Grolman, S. F. Klis, Neurotrophins and their role in the cochlea. *Hear. Res.* **288**, 19–33 (2012).
7. S. H. Green, E. Bailey, Q. Wang, R. L. Davis, The Trk A, B, C's of neurotrophins in the cochlea. *Anat. Rec.* **295**, 1877–1895 (2012).
8. Q. Yu, Q. Chang, X. Liu, Y. Wang, H. Li, S. Gong, K. Ye, X. Lin, Protection of spiral ganglion neurons from degeneration using small-molecule TrkB receptor agonists. *J. Neurosci.* **33**, 13042–13052 (2013).
9. O. Akil, R. P. Seal, K. Burke, C. Wang, A. Alemi, M. During, R. H. Edwards, L. R. Lustig, Restoration of hearing in the VGLUT3 knockout mouse using virally mediated gene therapy. *Neuron* **75**, 283–293 (2012).
10. K. Kawamoto, S. Ishimoto, R. Minoda, D. E. Brough, Y. Raphael, *Math1* gene transfer generates new cochlear hair cells in mature guinea pigs in vivo. *J. Neurosci.* **23**, 4395–4400 (2003).
11. M. Izumikawa, R. Minoda, K. Kawamoto, K. A. Abrashkin, D. L. Swiderski, D. F. Dolan, D. E. Brough, Y. Raphael, Auditory hair cell replacement and hearing improvement by *Atoh1* gene therapy in deaf mammals. *Nat. Med.* **11**, 271–276 (2005).
12. A. K. Wise, C. R. Hume, B. O. Flynn, Y. S. Jeelall, C. L. Suhr, B. E. Sgro, S. J. O'Leary, R. K. Shepherd, R. T. Richardson, Effects of localized neurotrophin gene expression on spiral ganglion neuron resprouting in the deafened cochlea. *Mol. Ther.* **18**, 1111–1122 (2010).
13. A. K. Wise, T. Tu, P. J. Atkinson, B. O. Flynn, B. E. Sgro, C. Hume, S. J. O'Leary, R. K. Shepherd, R. T. Richardson, The effect of deafness duration on neurotrophin gene therapy for spiral ganglion neuron protection. *Hear. Res.* **278**, 69–76 (2011).
14. P. J. Atkinson, A. K. Wise, B. O. Flynn, B. A. Nayagam, C. R. Hume, S. J. O'Leary, R. K. Shepherd, R. T. Richardson, Neurotrophin gene therapy for sustained neural preservation after deafness. *PLOS One* **7**, e52338 (2012).
15. S. P. Gubbels, D. W. Woessner, J. C. Mitchell, A. J. Ricci, J. V. Brigande, Functional auditory hair cells produced in the mammalian cochlea by in utero gene transfer. *Nature* **455**, 537–541 (2008).
16. M. Parker, A. Brugeaud, A. S. B. Edge, Primary culture and plasmid electroporation of the murine organ of Corti. *J. Vis. Exp.* **36**, 1685 (2010).
17. J. M. Jones, M. Montcouquiol, A. Dabdoub, C. Woods, M. W. Kelley, Inhibitors of differentiation and DNA binding (Ids) regulate Math1 and hair cell formation during the development of the organ of Corti. *J. Neurosci.* **26**, 550–558 (2006).
18. M. Masuda, K. Pak, E. Chavez, A. F. Ryan, TFE2 and GATA3 enhance induction of POU4F3 and myosin VIIa positive cells in nonsensory cochlear epithelium by ATOH1. *Dev. Biol.* **372**, 68–80 (2012).
19. H. Versnel, M. J. Agterberg, J. C. de Groot, G. F. Smoorenburg, S. F. Klis, Time course of cochlear electrophysiology and morphology after combined administration of kanamycin and furosemide. *Hear. Res.* **231**, 1–12 (2007).
20. N. Mersmann, D. Tkachev, R. Jelinek, P. T. Röth, W. Möbius, T. Ruhwedel, S. Rühle, W. Weber-Fahr, A. Sartorius, M. Klugmann, Aspartoacylase-lacZ knockin mice: An engineered model of Canavan disease. *PLOS One* **6**, e20336 (2011).
21. J. Gehl, Electroporation: Theory and methods, perspectives for drug delivery, gene therapy and research. *Acta Physiol. Scan.* **177**, 437–447 (1993).
22. S. Orlowski, L. M. Mir, Cell electropermeabilization: A new tool for biochemical and pharmacological studies. *Biochim. Biophys. Acta* **1154**, 51–63 (1993).
23. J. Teissie, M. Golzio, M. P. Rols, Mechanisms of cell membrane electropermeabilization: A minireview of our present (lack of ?) knowledge. *Biochim. Biophys. Acta* **1724**, 270–280 (2005).
24. M. P. Rols, Electropermeabilization, a physical method for the delivery of therapeutic molecules into cells. *Biochim. Biophys. Acta* **1758**, 423–428 (2006).
25. S. I. Sukharev, V. A. Klenchin, S. M. Serov, L. V. Chernomordik, A. Chizmadzhev Yu, Electroporation and electrophoretic DNA transfer into cells. The effect of DNA interaction with electropores. *Biophys. J.* **63**, 1320–1327 (1992).
26. D. Greenwood, D. J. Jagger, L. Huang, N. Hoya, P. R. Thorne, S. S. Wildman, B. F. King, K. Pak, A. F. Ryan, G. D. Housley, P2X receptor signaling inhibits BDNF-mediated spiral ganglion neuron development in the neonatal rat cochlea. *Development* **134**, 1407–1417 (2007).
27. T. G. Landry, A. K. Wise, J. B. Fallon, R. K. Shepherd, Spiral ganglion neuron survival and function in the deafened cochlea following chronic neurotrophic treatment. *Hear. Res.* **282**, 303–313 (2011).
28. J. M. Miller, C. G. Le Prell, D. M. Prieskorn, N. L. Wys, R. A. Altschuler, Delayed neurotrophin treatment following deafness rescues spiral ganglion cells from death and promotes regrowth of auditory nerve peripheral processes: Effects of brain-derived neurotrophic factor and fibroblast growth factor. *J. Neurosci. Res.* **85**, 1959–1969 (2007).
29. L. S. Kim, S. W. Jeong, Y. M. Lee, J. S. Kim, Cochlear implantation in children. *Auris Nasus Larynx* **37**, 6–17 (2010).
30. B. C. Thompson, R. T. Richardson, S. E. Moulton, A. J. Evans, S. O'Leary, G. M. Clark, G. G. Wallace, Conducting polymers, dual neurotrophins and pulsed electrical stimulation—Dramatic effects on neurite outgrowth. *J. Control. Release* **141**, 161–167 (2010).
31. D. R. Merrill, M. Bikson, J. G. Jefferys, Electrical stimulation of excitable tissue: Design of efficacious and safe protocols. *J. Neurosci. Methods* **141**, 171–198 (2005).
32. H. L. Fitzsimons, R. J. Bland, M. J. During, Promoters and regulatory elements that improve adeno-associated virus transgene expression in the brain. *Methods* **28**, 227–236 (2002).
33. S. M. Stoll, C. R. Sclimenti, E. J. Baba, L. Meuse, M. A. Kay, M. P. Calos, Epstein–Barr virus/human vector provides high-level, long-term expression of $\alpha_1$-antitrypsin in mice. *Mol. Ther.* **4**, 122–129 (2001).

34. M. J. Agterberg, H. Versnel, L. M. van Dijk, J. C. de Groot, S. F. Klis, Enhanced survival of spiral ganglion cells after cessation of treatment with brain-derived neurotrophic factor in deafened guinea pigs. *J. Assoc. Res. Otolaryngol.* **10**, 355–367 (2009).
35. A. H. Nagahara, M. H. Tuszynski, Potential therapeutic uses of BDNF in neurological and psychiatric disorders. *Nat. Rev. Drug Discov.* **10**, 209–219 (2011).
36. M. S. Hildebrand, S. S. Newton, S. P. Gubbels, A. M. Sheffield, A. Kochhar, M. G. de Silva, H. H. Dahl, S. D. Rose, M. A. Behlke, R. J. Smith, Advances in molecular and cellular therapies for hearing loss. *Mol. Ther.* **16**, 224–236 (2008).
37. C. Hamani, Y. Temel, Deep brain stimulation for psychiatric disease: Contributions and validity of animal models. *Sci. Transl. Med.* **4**, 142rv8 (2012).
38. B. A. West, R. E. Brummett, D. L. Himes, Interaction of kanamycin and ethacrynic acid. Severe cochlear damage in guinea pigs. *Arch. Otolaryngol.* **98**, 32–37 (1973).
39. R. T. Richardson, A. K. Wise, B. C. Thompson, B. O. Flynn, P. J. Atkinson, N. J. Fretwell, J. B. Fallon, G. G. Wallace, R. K. Shepherd, G. M. Clark, S. J. O'Leary, Polypyrrole-coated electrodes for the delivery of charge and neurotrophins to cochlear neurons. *Biomaterials* **30**, 2614–2624 (2009).
40. J. M. Cederholm, K. E. Froud, A. C. Wong, M. Ko, A. F. Ryan, G. D. Housley, Differential actions of isoflurane and ketamine-based anaesthetics on cochlear function in the mouse. *Hear. Res.* **292**, 71–79 (2012).
41. H. Aihara, J. Miyazaki, Gene transfer into muscle by electroporation in vivo. *Nat. Biotechnol.* **16**, 867–870 (1998).

**Acknowledgments:** We thank J. Patrick and P. Carter from Cochlear Ltd. for advice on the project, and T.-T. Hung and A. Kwek from the University of New South Wales Biological Resources Imaging Laboratory and the National Imaging Facility of Australia for supporting the micro–computed tomography imaging of the cochlear implant electrode array. **Funding:** The work was supported by Australian Research Council Linkage grant LP0992098, which included co-funding by Cochlear Ltd. (Australia). Cochlear Ltd. also supported the study with materials, including the cochlear implant electrode arrays. J.L.P. was supported by an Australian Postgraduate Award. **Author contributions:** J.L.P. contributed to all parts of the study design, experimental work, data analysis, and manuscript preparation. S.F.T. contributed particularly to the cochlear implant surgeries, deafening model, and histology. S.F.T., K.E.F., A.C.Y.W., I.T.T., E.N.C., and M. Ko contributed to the development of the CFE and cochlear implant experiments. R.M. and M. Klugmann contributed to the gene construct development, experimental design, analysis, and manuscript preparation. G.D.H. led the project and the manuscript production. **Competing interests:** Two patent filings are associated with this research: (i) Title: Method of providing agents to the cochlea. Inventor: G. D. Housley. Filing status: National Phase Examination—Europe (application no. 10799287.7; filing date 5 July 2010), National Phase—United States (application no. 13/384020; filing date 5 July 2010). Assignee: NewSouth Innovations Pty Limited. (ii) Title: Method and apparatus for close-field electroporation. Inventor: G. D. Housley, M. Klugmann, J. Pinyon. Filing status: Provisional, Australia (application no. 2013902263; filed 21 June 2013). Assignee: NewSouth Innovations Pty Limited. **Data and materials availability:** For transfer of plasmid-based materials, a materials transfer agreement is required.

Submitted 2 December 2013
Accepted 7 March 2014
Published 23 April 2014
10.1126/scitranslmed.3008177

**Citation:** J. L. Pinyon, S. F. Tadros, K. E. Froud, A. C. Y. Wong, I. T. Tompson, E. N. Crawford, M. Ko, R. Morris, M. Klugmann, G. D. Housley, Close-field electroporation gene delivery using the cochlear implant electrode array enhances the bionic ear. *Sci. Transl. Med.* **6**, 233ra54 (2014).